



SUNLIBB

Sustainable Liquid Biofuels from Biomass Biorefining

Grant Agreement no. 251132

Collaborative Project
EU 7th Framework Programme
ENERGY

Project duration: 1st October 2010 – 30th September 2014

Deliverable 4.4

“Metabolic maps for maize, integrating transcripts, metabolites and altered fluxes”

Authors: **Prof. Wout Boerjan (VIB University of Ghent)**

Workpackage: **4**

Workpackage Leader: **Prof. Wout Boerjan (VIB U.Ghent)**

Due date: **September 2013 (Project month 36)**

Actual submission date: **March 2014**

Re-formatted version submitted: **December 2014**

Dissemination Level: **PU**

SUNLIBB deliverables

Del No: 4.4	Deliverable Name: Metabolic maps for maize, integrating transcripts, metabolites and altered fluxes			
WP: 4	Lead partner: P12	Dissemination level: PU	Delivery date (proj month): 36	Actual delivery date: Month 42

Objective:

A tight feedback of lignin perturbation on the phenylpropanoid pathway has been shown in the dicot model plant, *Arabidopsis* (Vanholme *et al.*, 2010; 2012). Here, it is our objective to obtain insights into the response of the phenylpropanoid pathway to lignin perturbation in maize. Therefore, maize lines mutated in *C4H* and *CAD* were studied, using a combined approach involving biochemical, transcriptomic and metabolomic analyses.

Results:

Transcriptomic and metabolomic studies were performed on a set of lignin mutants in genes *ZmCCR1*, *ZmC4H1* and *ZmCAD2* (described in Deliverable 1.6). Biogemma (Partner 3) produced the material in the field. Six replicates of 20 to 25 plants per entry were included in the experiment for each of the 4 sampled developmental stages. A bulk sample of the growing internode below the main ear from 5 to 10 different plants was taken at each of the 4 stages: V10 (collar of leaf number 10 is visible), S (silking stage), S+7D (silking stage + 7 days), S+14D (silking stage + 14 days). Six and four replicates were used for the metabolomic and transcriptomic assays, respectively. The design is illustrated in figure 1.

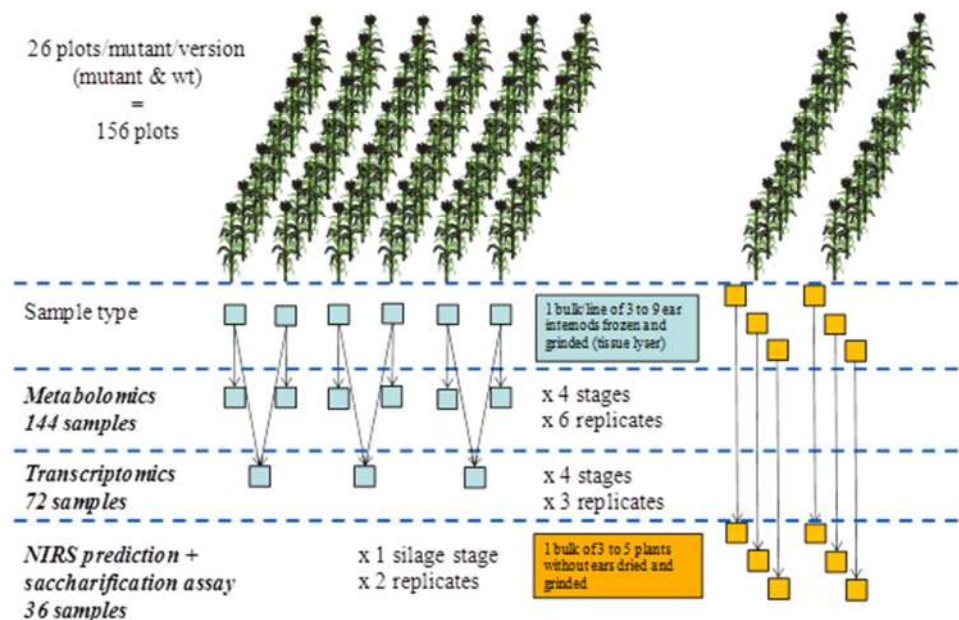


Figure 1: Experimental design

Zmccr1 appeared to have lost its intended mutation, so the generated data were therefore not investigated further. In contrast, both *zmc4h1* and *zmcad2* mutants appeared very valuable lines for further investigation. For the comparison of gene expression in *zmc4h1* mutant and control plants,

only the V10 stage was considered, because *zmc4h1* mutant plants showed a delay in development in the later S, S+7d and S+14d stages, which compromised correct interpretation of these data. First, the effect of *ZmC4H1* perturbation on the expression of genes within the same pathway was analyzed. The log₂ fold changes in expression of the phenylpropanoid genes in the *zmc4h1* mutant versus control plants that were anticipated to be involved in lignification can be found in Table 1. The perturbation of *ZmC4H1* caused the up-regulation of all phenylpropanoid genes (except for the *CCR* gene) that were selected as being putatively involved in lignification. Moreover, for the gene families of *C4H*, *4CL*, *C3H*, *CCoAOMT* and *CAD*, specifically those genes that were selected to be involved in lignification showed the highest response to *ZmC4H1* perturbation, further strengthening this assumption. Furthermore, it is noteworthy that the presence of the transposon in the first intron of the *ZmC4H1* gene did not cause a reduction in transcript abundance, in contrast, it increased in abundance.

*Table 1. Log₂ fold changes in expression levels of phenylpropanoid genes that were selected for high and increasing expression over development in control plants were compared in *zmc4h1* mutant as compared to control. Fold changes are colour-coded according to higher (red) and lower (blue) in *zmc4h1* mutant samples in V10 stage (ten visible leaf collars).*

protein name	log ₂ fold change (mutant vs. control) in V10 stage
PAL	0.36
PAL	0.48
PAL	0.63
PAL	0.79
PAL	0.96
PAL	0.49
C4H	0.82
4CL	0.54
HCT	0.66
HCT	0.23
C3H	0.66
CCoAOMT	0.88
CCoAOMT	1.06
CCoAOMT	0.86
CCR	0.00
F5H	0.33
COMT	1.02
CAD	0.74

To investigate whether *ZmCAD2* perturbation affected expression of genes within the same pathway, fold changes in gene expression in the *zmcad2* mutant compared to control samples were determined (Table 2). In contrast to the *zmc4h1* mutant, no major changes in expression levels were present in the V10 stage of *zmcad2* mutants, except *ZmCAD2* itself (GRMZM2G110175) which was highly down-regulated. As the transposon is situated in an exon, proper transcription of the *ZmCAD2* gene would thus be abolished. In the reproductive stages S, S+7d and S+14d, several genes were up-regulated in the *zmcad2* mutant. The highest up-regulated genes were *ZmC4H1* and *ZmF5H1* in the S+7d stage. The perturbation of *ZmCAD2* thus appears to cause up-regulation of lignin genes. In

addition, two other *CAD* genes that were only moderately and weakly expressed in control internodes showed strong up-regulation in the *zmcad2* mutant.

Table 2. Log2 fold changes in expression levels of phenylpropanoid genes with high and increasing expression over development in zmcad2 mutant, as compared to control. Fold changes are colour-coded according to higher (red) and lower (blue) transcript levels in zmcad2 mutant samples in four stages of development: V10 (ten visible leaf collars), S (silking), S+7d (seven days after silking) and S+14d (fourteen days after silking).

protein functio	log2 fold change (mutant vs. control)			
	V10	S	S+7d	S+14d
PAL	-0.24	0.14	0.18	0.07
PAL	0.06	0.34	0.22	0.31
PAL	-0.13	0.25	0.16	-0.03
PAL	-0.14	0.15	0.34	0.15
PAL	-0.08	0.03	0.15	0.22
PAL	-0.06	0.39	0.04	-0.30
C4H	-0.04	0.55	0.97	0.23
4CL	-0.26	0.48	-0.75	0.12
HCT	-0.13	0.32	-0.17	0.09
HCT	-0.07	-0.09	-0.08	0.15
C3H	-0.14	0.39	0.60	-0.03
CCoAOMT	0.02	-0.11	0.20	0.67
CCoAOMT	-0.27	0.24	-0.08	0.36
CCoAOMT	-0.01	0.08	-0.11	0.19
CCR	0.20	0.00	0.10	0.44
F5H	-0.03	-0.12	0.98	0.26
COMT	-0.18	0.41	0.28	0.28
CAD	-2.28	-1.43	-1.04	-0.82

In order to investigate the general effects of *ZmC4H1* perturbation on gene expression levels beyond the already investigated phenylpropanoid pathway, a GO enrichment analysis was performed using the differentially expressed probes in the V10 stage. For the GO enrichment analysis, the web-based Gene Ontology Enrichment Analysis Software Toolkit (GOEAST) was used. This tool allowed GO enrichment analysis from custom micro-arrays, which was the case in our study. A total of 103 GO categories were significantly ($p_FDR < 0.05$) enriched in *zmc4h1* internodes in the V10 stage (Table 3). Several highly enriched GO categories can be related to the perturbation of the *ZmC4H1* gene: cinnamic acid biosynthetic and metabolic process, plant-type cell wall biogenesis, benzene-containing compound metabolic process, phenylpropanoid biosynthetic and metabolic process, secondary metabolic process and secondary metabolite biosynthetic process.

Table 3. Heat map showing the enrichment in Gene ontology (GO) terms in *zmc4h1* mutant internodes in V10 stage using GOEAST (<http://omicslab.genetics.ac.cn/GOEAST/>). The p-value of GO enrichment is calculated as the hypergeometric probability to get so many probes for a GO term, under the null hypothesis that they were picked out randomly from the microarray. In this heat map, the Log odds-ratio (LR) is shown for significant enriched GO terms. Basically, the bigger the LR, the higher the relative abundance of this GO term is compared to random situation.

GO category name	log odss-ratio	p-value	GO category name	log odss-ratio	p-value
1 cinnamic acid biosynthetic process	3.467	4.E-02	37 response to temperature stimulus	1.692	1.E-02
2 cinnamic acid metabolic process	3.467	4.E-02	38 anatomical structure morphogenesis	1.650	2.E-03
3 DNA geometric change	3.315	3.E-03	39 response to endogenous stimulus	1.586	6.E-03
4 DNA duplex unwinding	3.315	3.E-03	40 cellular response to chemical stimulus	1.564	1.E-02
5 plant-type cell wall biogenesis	2.730	4.E-02	41 reproductive structure development	1.534	3.E-03
6 response to sucrose stimulus	2.637	4.E-02	42 reproductive system development	1.534	3.E-03
7 response to disaccharide stimulus	2.637	4.E-02	43 macromolecule methylation	1.516	8.E-03
8 benzene-containing compound metabolic process	2.611	2.E-02	44 developmental process involved in reproduction	1.506	1.E-03
9 copper ion transport	2.467	2.E-02	45 post-embryonic development	1.495	1.E-03
10 defense response to fungus	2.400	4.E-02	46 response to hormone stimulus	1.481	3.E-02
11 phenylpropanoid biosynthetic process	2.315	1.E-02	47 response to organic substance	1.476	1.E-03
12 nucleic acid phosphodiester bond hydrolysis	2.297	4.E-02	48 methylation	1.473	5.E-05
13 phenylpropanoid metabolic process	2.270	2.E-04	49 anatomical structure development	1.447	1.E-04
14 regulation of flower development	2.154	8.E-03	50 system development	1.443	5.E-04
15 secondary metabolic process	2.141	1.E-06	51 aromatic compound catabolic process	1.398	3.E-04
16 anatomical structure formation involved in morphogenesis	2.085	1.E-02	52 developmental process	1.368	1.E-05
17 regulation of reproductive process	2.085	1.E-02	53 single-organism developmental process	1.367	2.E-03
18 secondary metabolite biosynthetic process	2.080	3.E-03	54 ribosome biogenesis	1.367	2.E-03
19 regulation of multicellular organismal process	2.076	1.E-03	55 organic cyclic compound catabolic process	1.358	4.E-04
20 regulation of multicellular organismal development	2.076	1.E-03	56 negative regulation of biological process	1.339	5.E-02
21 regulation of post-embryonic development	2.052	1.E-02	57 ribonucleoprotein complex biogenesis	1.325	3.E-03
22 regulation of developmental process	1.964	1.E-03	58 rRNA processing	1.297	4.E-02
23 organ morphogenesis	1.914	5.E-02	59 reproductive process	1.295	1.E-02
24 protein methylation	1.867	4.E-02	60 rRNA metabolic process	1.286	4.E-02
25 protein alkylation	1.867	4.E-02	61 multicellular organismal development	1.250	4.E-04
26 post-embryonic organ development	1.839	4.E-02	62 response to abiotic stimulus	1.203	3.E-03
27 Golgi vesicle transport	1.811	4.E-02	63 heterocycle catabolic process	1.166	5.E-02
28 flower development	1.811	4.E-02	64 cellular nitrogen compound catabolic process	1.166	5.E-02
29 positive regulation of biological process	1.799	3.E-03	65 cellular polysaccharide metabolic process	1.122	2.E-02
30 tissue development	1.793	1.E-02	66 response to chemical stimulus	1.113	3.E-04
31 organ development	1.766	2.E-04	67 oxidation-reduction process	1.026	2.E-11
32 cellular response to hormone stimulus	1.754	4.E-02	68 ncRNA metabolic process	1.012	4.E-02
33 cellular response to endogenous stimulus	1.754	4.E-02	69 transcription, DNA-dependent	0.888	1.E-02
34 cellular response to organic substance	1.712	9.E-03	70 RNA biosynthetic process	0.875	1.E-02
35 cell differentiation	1.708	4.E-02	71 RNA metabolic process	0.695	4.E-04
36 response to oxygen-containing compound	1.707	2.E-04	72 single-organism metabolic process	0.349	1.E-03

In secondary metabolism, genes related to synthesis of terpenoids, chalcones, flavones, flavonols and anthocyanidins were highly but adversely affected in gene expression. While chalcone, flavonol and anthocyanidin synthesis were up-regulated, terpenoid synthesis was down-regulated. It is notable that genes encoding enzymes that are known to act in the formation of flavonoids were highly upregulated. These are formed from *p*-coumaroyl CoA which is produced by 4CL from *p*-coumaric acid, the direct product of C4H. The first steps of the biosynthetic pathway from *p*-coumaroyl CoA to flavonoids involve the action of chalcone synthase (CHS) and chalcone isomerase (CHI) to produce the flavanone Naringenin. From Naringenin, the pathway branches off towards isoflavones by the action of isoflavone synthases (IFS) and further on involves an isoflavone reductase (IFR). Also from Naringenin, flavanones and flavonols are produced by the action of Flavanone 3-hydroxylase (F3H) and flavanone 3'-5'-hydroxylase (F3'H) (Figure 2). From here, the pathway branches off again into flavonols by the action of flavonol synthase (FLS) and into anthocyanidins by the action of dihydroflavonol 4-reductase (DFR) (Sharma *et al.* 2012). Genes encoding 4CL, CHS, CHI, FLS and DFR were all found to be up-regulated in *zmc4h1* internodes. The up-regulation is moderate (0-2 log fold change) for 4CL and FLS and high (>2 log fold change) for CHS, CHI and DFR (Figure 4). The expression of one DFR gene is the second highest upregulated gene among all significantly differentially expressed genes in V10 in *zmc4h1*. A similar experiment has been completed for the ZMCAD2 mutant, but data is not shown, due to space limitations.

Next, the metabolites that were previously identified via the CSPP algorithm (presented in deliverable 4.3) were mapped on a metabolic pathway. Subsequently, their abundance in the mutants as compared to the abundance in wild type plants was calculated and appropriate statistics were applied. Then, their relative abundances were mapped on the metabolic pathways (as shown in figure 3 and 4), to aid interpretation of the data.

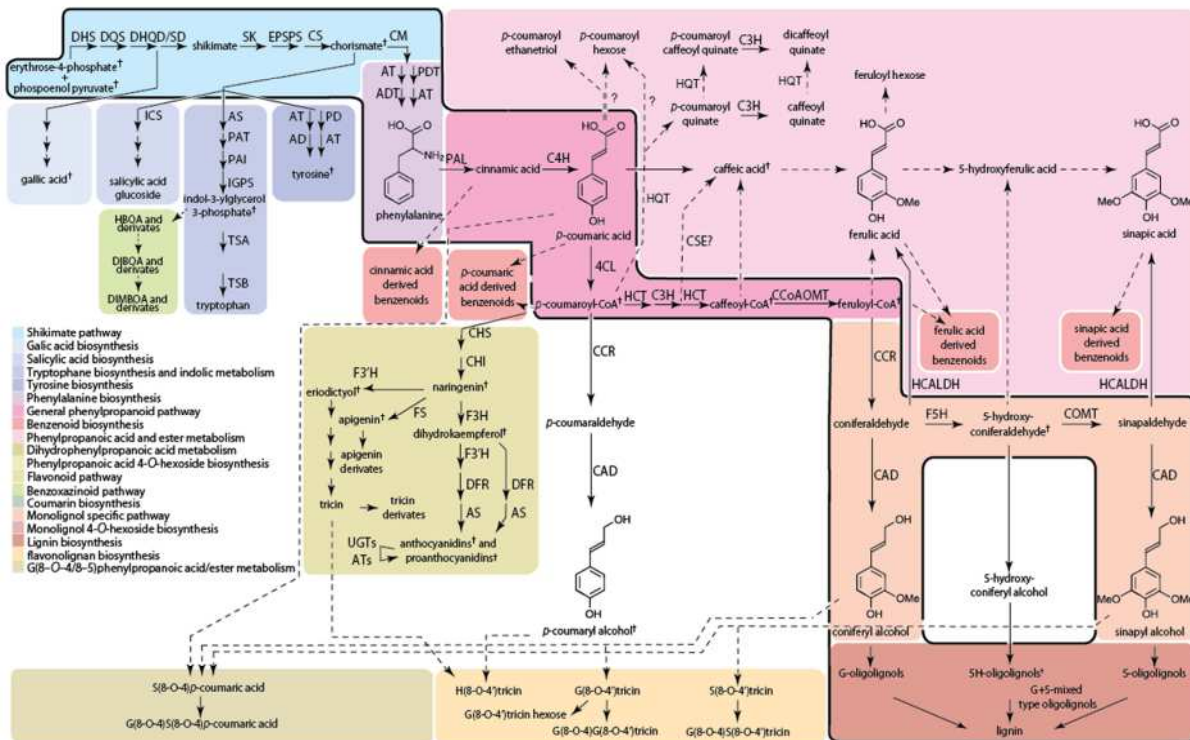


Figure 2: Metabolic map of the phenylpropanoid biosynthesis in Maize

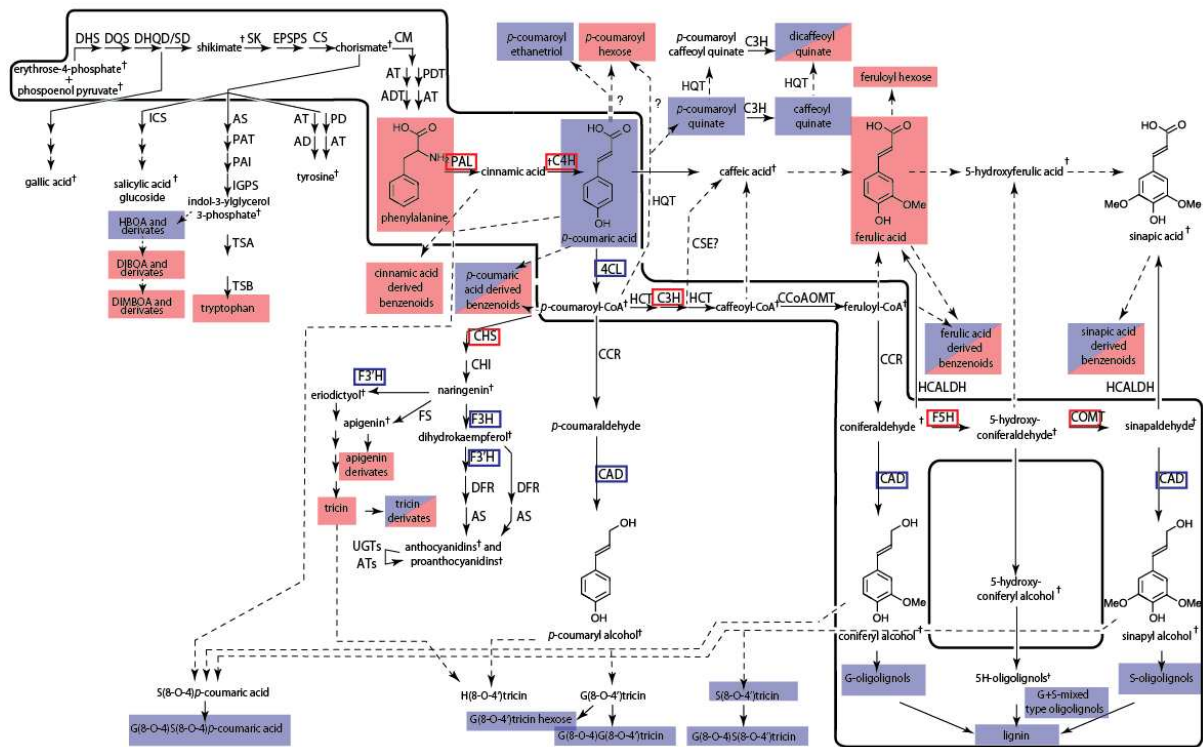


Figure 3: Metabolic shifts in phenolic metabolism at the S+7 stage, as a result of a mutation of ZMCAD. The relative increase and decrease of transcript and metabolite abundances in each of the mutants, as compared to wild type, was mapped manually on the pathway as discrete features. Differences in metabolites are indicated via boxes, where red represents a significant increase and blue a significant decrease in abundance. Differences in transcript abundance are indicated with right-angled, framed boxes: significant increases and decreases are visualized via red and blue boxes with solid borders.

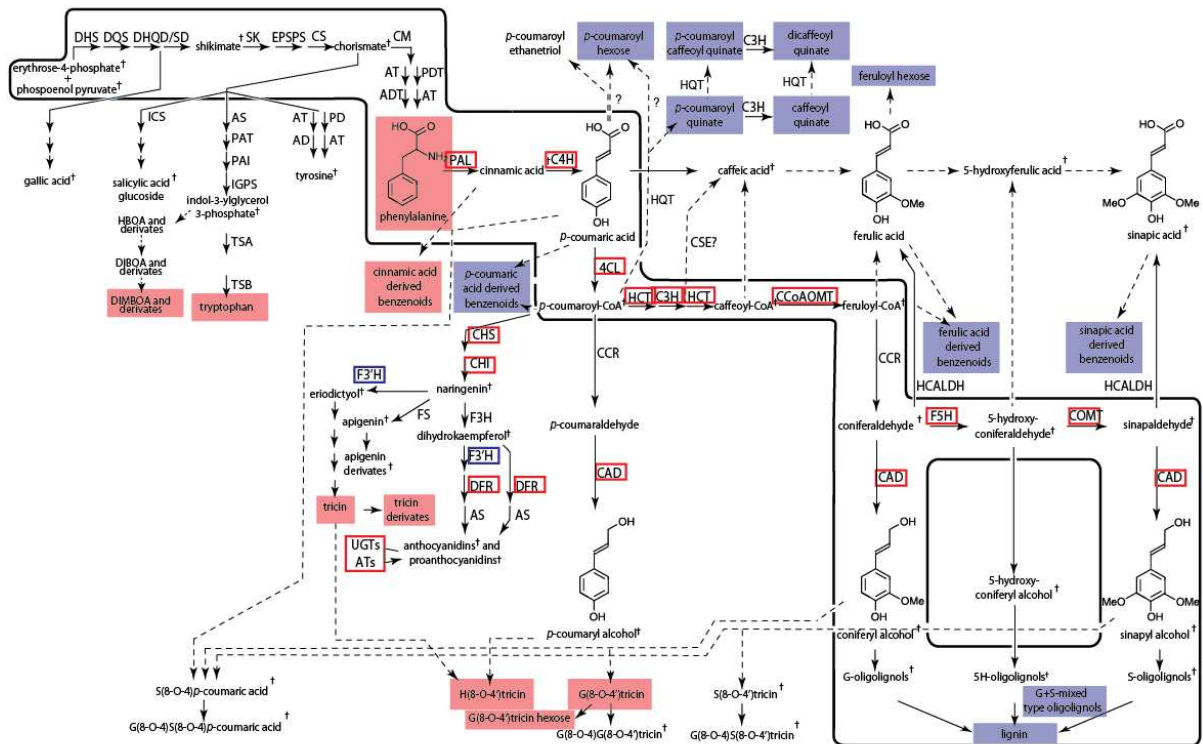


Figure 4: Metabolic shifts in phenolic metabolism at the V10 stage, as a result of a mutation of ZmC4H. The relative increase and decrease of transcript and metabolite abundances in each of the mutants, as compared to wild type, was mapped manually on the pathway as discrete features. Differences in metabolites are indicated via boxes, where red represents a significant increase and blue a significant decrease in abundance. Differences in transcript abundance are indicated with right-angled, framed boxes: significant increases and decreases are visualized via red and blue boxes with solid borders.

Discussion /Conclusion:

Maize lines mutated in *ZmC4H* and *ZmCAD2* were studied via the combined use of biochemical, transcriptomic and metabolomic analysis. Metabolic maps were generated and the metabolic shifts in the different mutants were visualized on the maps. The results provide valuable insight into phenylpropanoid metabolism. For example, in accordance with current pathway knowledge, the flux towards lignin, *p*-coumaroyl and caffeoyl quinates is clearly hindered in *zmc4h* mutants. Surprisingly, the flux towards flavonoids and flavonolignans is favoured, suggesting either a specific feedback regulation or that enzymatic steps are missing in our current pathway model (e.g. flavonoids from cinnamoyl-CoA). We are currently preparing two manuscripts, one about the effects of *zmc4h* mutation and one about the effects of mutating *ZmCAD*.

References:

- Berthet S, Thevenin J, Baratiny D, *et al.* (2012) Role of Plant Laccases in Lignin Polymerization, 1st ed. Lignins 61:145-172. doi: 10.1016/B978-0-12-416023-1.00005-7
- Caparrós-Ruiz D, Fornalé S, Civardi L, *et al.* (2006) Isolation and characterisation of a family of laccases in maize. Plant Science 171:217-225. doi: 10.1016/j.plantsci.2006.03.007
- Sharma M, Chai C, Morohashi K, *et al.* (2012) Expression of flavonoid 3'-hydroxylase is controlled by P1, the regulator of 3-deoxyflavonoid biosynthesis in maize. BMC plant biology 12:196. doi: 10.1186/1471-2229-12-196
- Vanholme *et al.*, 2010 Engineering traditional monolignols out of lignin by concomitant up-regulation of F5H1 and down-regulation of COMT in Arabidopsis. The plant journal 64(6) 885-897
- Vanholme *et al.*, 2012 A Systems Biology View of Responses to Lignin Biosynthesis Perturbations in Arabidopsis. The Plant Cell 24(9) 3506-3529